LargeBRAT: Complex Backward Reach-Avoid Tubes. An Emergent Collective Behavior Framework.

Olalekan Ogunmolu

Microsoft Research, NYC, 300 Lafayette Street, New York, NY 10012, USA
lekanmolu@microsoft.com.

Abstract. Hitherto, the numerical verification of *complex* and *nonlinear* systems via the Isaacs equation (with an overapproximation guarantee of the backward reachable set or tube) has proven elusive owing to the exponential computational complexity associated with resolving value functions on a mesh. In this work, we present a globally isotropic yet locally anisotropic reachable set/tube computational scheme, aimed at computating the backward reach-avoid-tubes (BRATs) of multiple agents interacting over a large state space. This is achieved by resolving the extrema of payoffs on local substructures of the state space whilst preserving desirable global payoff properties. Within the bounds here set, our scheme presents a simple yet effective strategy for designing the verification of *nonlinear systems* via large backward reach-avoid sets or tubes.

1 INTRODUCTION

In multi-agent systems, the interconnection among subsystems can be characterized as moving interfaces, boundaries of local regions or cells that interact, or mixing of interacting organism substructures. The kinematics and kinetics of such systems involve topologically complex domain reformulation which are often difficult to resolve in a conceptual, computational, and numerically robust manner.

In this paper, we will establish a general theorem for systems that exhibit the structural properties described in the foregoing for the practical verification of complex nonlinear systems whose global dynamical evolution is an aggregation of multiple local kinematics and kinetics that emerge collectively across the subsystems or regions of a large state space. With Bolza-type objective functionals and backward reachability theory, we will aggregate the over-approximated backward reach avoid tubes or sets (BRATs) of the respective subsystems across space and time scales. To achieve this goal, we will leverage our understanding of flocking in natural swarms, particularly European starlings (*Sturnus vulgaris*), as well as rely on tools from level set methods [1, 2]. Applications of the principles described herein may include the verification of cyber-physical systems or CPS, multi-agent robotic systems requiring dynamical dexterity [3], or dynamical systems with locally valid asymptotic controllers that do not admit a continuous control law for arriving at a globally asymptotically stable solution [4, Theorem II]. Mostly, we will work locally in our formulations, but occasionally will make global remarks.

Differential optimal control theory and games offer a useful paradigm for resolving the safety of multiple agents interacting over a large shared space. Both rely on the

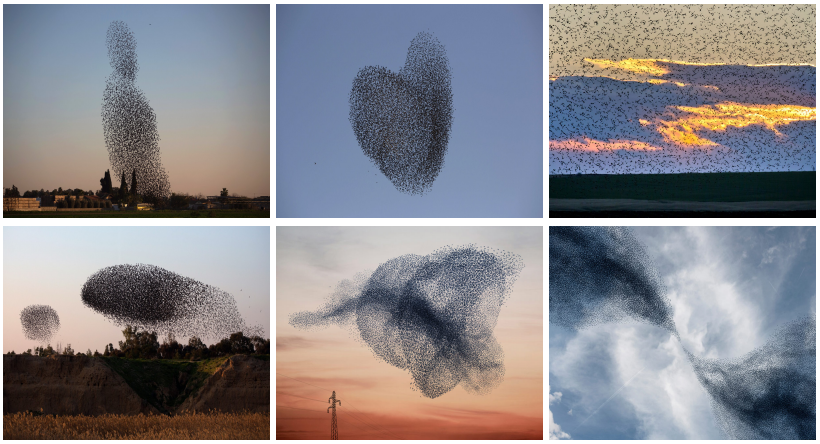

Fig. 1: Starlings murmurations. From the top-left and clockwise. (i) A starlings flock rises into the air, in a dense structure (Reuters/Amir Cohen). (ii) Starlings migrating over an Israeli village (AP Photo/Oded Balilty). (iii) Starlings feeding on laid seeds in the ground in Romania. (iv) Two flocks of migrating starlings (Menahem Kahana/AFP/Getty Images). (v) A concentric conical formation of starlings (Courtesy of The Gathering Site.). (vi) Splitting and joining of a flock of starlings.

resolution of the Hamilton-Jacobi-Bellman (HJB) equation or its Isaacs counterpart (HJI). As HJ-type equations are seldom regular enough to admit a classical solution for almost all *practical* problems, "weaker" or "viscosity" solutions [5–7] provide generalized solutions to HJ partial differential equations (P.D.E.s) under relaxed regularity conditions; these viscosity solutions are not necessarily differentiable anywhere in the state space, and the only regularity prerequisite in the definition is continuity [8]. However, wherever they are differentiable, they satisfy the values of HJ P.D.E.s in a classical sense. Thus, they lend themselves well to many real-world problems existing at the interface of discrete, continuous, and hybrid systems [9–12].

With the elegant theoretical results of [6, 7, 13–15], stable essentially non-oscillatory Lax-Friedrichs numerical integration schemes provide *consistent* and *monotone* viscosity solutions (with high accuracy and precision *on a mesh*) to multi-dimensional HJ-type equations[1]. However, by discretizing the Hamiltonian on a dimension-by-dimension basis, the scheme suffers from scalability [16–18] as a result of the exponential computational complexity. Given the limits of computational resources and memory when resolving practical problems for multiagent systems, what if we exploit local structures within a complex system and resolve the overall Hamiltonian by an aggregation of the computation of the numerical fluxes of local Hamiltonians? This is the central question that this paper seeks to address.

[1] Consistent solutions to HJ equations are those whose explicit marching schemes via discrete approximations to the HJ IVP agree with the nonlinear HJ solution [14]. Such schemes are said to be *monotone* e.g. on $[-\mathbb{R}, \mathbb{R}]$ if the numerical approximation to the vector field of interest is a nondecreasing function of each argument of the discrete approximation to the vector field.

Paper Goals: Our goal here is the verification of *complex* and *nonlinear* behavior of *multi-agent autonomous systems* that is robust against a worst-case disturbance, and preserves local safety objectives *under global cohesion goals*. We limit our scope to providing a framework for separately computing the extremals of local payoffs of state space substructures over as large a range of initial conditions as desired over a complex state space, and providing a means for aggregating such locally computed values at the end of each Lax-Friedrichs numerical integration scheme [14, 15]. We consider local control laws in separated partitions of the state space as a procedure for synthesizing the practical verification of nonlinear systems. By properly coordinating local control laws, coordinated influence across workspace regions can be exerted over a wider range. As a motivating example, we analyze the problem within the framework of two-person vehicular dynamics over a large state space.

Natural Swarms as an Inspiration: Natural swarms provide clues on efficiently constructing a game's outcome(s), Hamiltonians, control laws, and strategies that govern the transient behaviors of many systems that possess structural subsystems with the properties we have introduced in the foregoing. We now know that local flocks within large murmurations of starlings maintain an anisotropic formation based on a topological interaction, regardless of sparsity of birds within a flock [19]. Thus, intra- and inter-flock collision are avoided and attacks are fended off [20].

Through empirical [20–22] and theoretical findings [23], evidence now abounds that in certain natural species that exhibit collective behavior TO-DO: (see Fig. 1), convergence and group cohesion is based on simple topological interaction rules that they use to keep a tab on one another in *local flocks* for collision avoidance, preserving density and structure, flock splitting, vacuole, cordon, and flash expansion [24]. This helps these animals preserve an eye-pleasing local anisotropic synchrony, which taken together among possibly hundreds of thousands of local interactions[2] [24], keep these animals whirling, swooping, and flying in an isotropic formation [20]. Thus, individual agents aggregate into finite flocks, and flock motion is synergized via local topological interactions in order to realize a stable global heading and cohesion [23]. There exists evidence that when an individual within a flock of starlings senses danger (e.g. an attack from a Peregrine Falcon), it changes its course immediately. Owing to the lateral vision in such animals, immediate *nearest neighbors* change course in response. This information is propagated across the entire group of flocks within the fraction of a second [20], resulting in the beautiful formations TO-DO: c.f. Fig. 1.

While Jadbabaie et al. [23] introduced a graphical formulation based on a switched linear system to demonstrate that nearest neighbor rules cause agents to converge to the same heading, we stick with the nonlinear model of the system and employ *reachability analysis* as a verification tool. We introduce new insights, and computational techniques aimed at solving *practical* problems that cannot be otherwise analytically resolved nor numerically resolved without exploiting state substructures and parallelism. This work is the first to systematically provide a rational separated value function aggregation scheme on local state space substructures in computing *robustly controlled backward reachable tubes (RCBRTs)* [10] for complex systems. The body of this paper is structured

[2] It has been reported that no birds fly together with greater coordination and complexity than European starlings, with murmurations counting upwards of 750,000 individual birds!

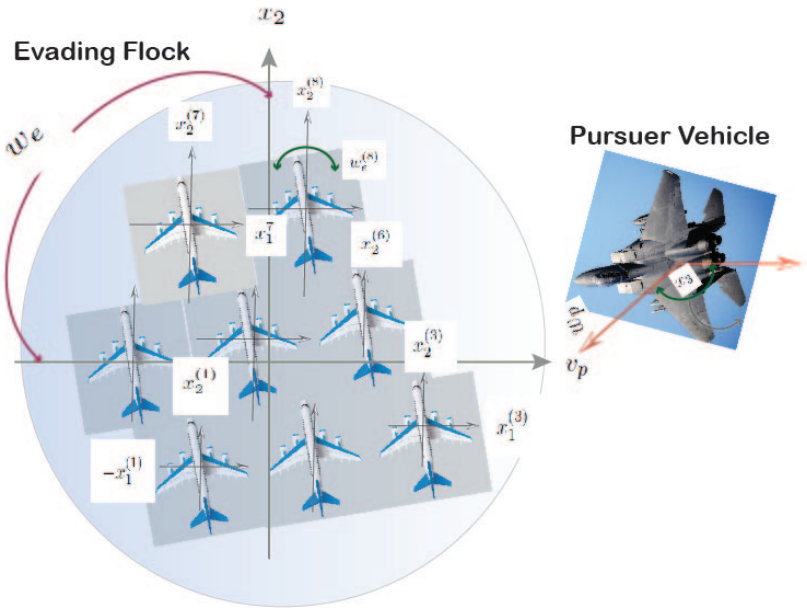

Fig. 2: Illustration of robust heading consensus for a flock with 8 aircraft. The evading player has all the evading agents under the will of its strategy. To every evading flock, there is at most one pursuing player.

as follows: we introduce common notations and definitions in § 2; § 3 describes the concepts and topics as needed for our proposed scheme in § 4; we present results and insights from experiments in § 5. Lastly, we conclude with remarks in § 6.

2 Notations and Definitions.

Let us now introduce the notations that are commonly used in this article. Time variables e.g. t, t_0, τ, T will always be real numbers. We let $t_0 \leq t \leq t_f$ denote fixed, ordered values of t. Vectors shall be column-wise stacked and be denoted by small bold-face letters i.e. $\mathbf{e}, \mathbf{u}, \mathbf{v}$ e.t.c. Matrices will be denoted by bold-math Latin upper case fonts e.g. $\mathbf{T}, \mathbf{S}$. Exceptions: the unit matrix is $\boldsymbol{I}$; and i, j, k, p are indices. Positive, negative, increasing, decreasing e.t.c. shall refer to strict corresponding property.

The set S of all $\boldsymbol{x}$ such that $\boldsymbol{x}$ belongs to the real numbers $\mathbb{R}$, and that $\boldsymbol{x}$ is positive shall be written as $S = \{\boldsymbol{x} \,|\, \boldsymbol{x} \in \mathbb{R}, \boldsymbol{x} > 0\}$. The cardinality of S shall be written as $[S]$. We define Ω as the open set in $\mathbb{R}^n$. To avoid the cumbersome phrase "the state $\boldsymbol{x}$ at time t", we will associate the pair $(\boldsymbol{x}, t)$ with the *phase* of the system for a state $\boldsymbol{x}$ at time t. Furthermore, we associate the Cartesian product of Ω and the space $T = \mathbb{R}^1$ of all time values as the *phase space* of $\Omega \times T$. The interior of Ω is denoted by $\text{int}\ \Omega$; whilst the closure of Ω is denoted $\bar{\Omega}$. We denote by $\delta\Omega\,(:= \bar{\Omega} \backslash \text{int}\ \Omega)$ the boundary of the set Ω.

Unless otherwise stated, vectors $\boldsymbol{u}(t)$ and $\boldsymbol{v}(t)$ are reserved for admissible control (resp. disturbance) at time t. We say $\boldsymbol{u}(t)$ (resp. $\boldsymbol{v}(t)$) is piecewise continuous in t, if

for each t, $\boldsymbol{u} \in \mathcal{U}$ (resp. $\boldsymbol{v} \in \mathcal{V}$), $\mathcal{U}($ resp. $\mathcal{V})$ is a Lebesgue measurable and compact set. At all times, any of $\boldsymbol{u}$ or $\boldsymbol{v}$ will be under the influence of a *player* such that the motion of a state $\boldsymbol{x}$ will be influenced by the will of that player. Our operational domain involves conflicting objectives between various agents e.g. with a heading convergence goal under an external disturbance' influence. For agents that are members of a local coordination group, collision avoidance shall apply so that agents within a local neighborhood cooperate to avoid entropy and preying pursuer(s). Thus, the problem at hand assumes that of a pursuit *game*. And by a game, we do not necessarily refer to a single game, but rather a *collection of games*. Such a game will terminate when *capture* occurs, that is the distance between players falls below a predetermined threshold.

Each player in a game shall constitute either a pursuer ($\boldsymbol{P}$) or an evader ($\boldsymbol{E}$). The cursory reader should not interpret $\boldsymbol{P}$ or $\boldsymbol{E}$ as controlling a single agent. In complex settings, we may have several pursuers (enemies) or evaders (peaceful citizens). However, when $\boldsymbol{P}$ or $\boldsymbol{E}$ governs the behavior of but one agent, these symbols will denote the agents themselves. The first component of an agent labeled say 5 within a flock labeled 2 is written $\boldsymbol{x}_1^{(5)_2}$. Each evading agent, identified by its label i as a state superscript, is parameterized by three state components: its linear velocities $(\boldsymbol{x}_1^{(i)}, \boldsymbol{x}_2^{(i)})$, and its heading $w^{(i)}$. When we need to distinguish an agent within a flock say F_j from another flock F_k, we shall use the index of the flock e.g. j as a further subscript for a particular agent's state i.e. $\boldsymbol{x}_1^{(i)_j} \neq \boldsymbol{x}_1^{(i)_k}$.

Given the various possibilities of outcomes, the question of what is "best" will be resolved by a *payoff*, Φ, whose extremal over a time interval will constitute a *value*, $\boldsymbol{V}$[3]. We adopt Isaac's [25] language so that if the payoff for a game is finite, we shall have a *game of kind*; and for a game with a continuum of payoffs, we shall have *a game of degree*. The *strategy* executed by $\boldsymbol{P}$ or $\boldsymbol{E}$ during a game shall be denoted by $\alpha \in \mathcal{A}$ (resp. $\beta \in \mathcal{B}$). With this definition, a control law e.g. $\boldsymbol{u}^{(i)}$ played by a player e.g. $\boldsymbol{P}$ will affect *agent* i; and a collection of agents under $\boldsymbol{P}$'s *willpower* be referred to as a *flock*. We shall refer to an aggregation of flocks on a state space as a *murmuration* [4].

3 Reachability for Systems Verification.

A basic characteristic of a control system is to determine the point sets within the state space that are *reachable* with a control input choice. An example objective in *reachability analysis* could be a target ($\mathcal{L}$) protection objective by an evading player from a pursuing player. Our treatment here is a special case of Isaac's homicidal chauffeur's game [25], whereupon $\boldsymbol{P}$ and $\boldsymbol{E}$ travel at constant linear speeds but have different headings, e.g. where the $\boldsymbol{P}$ seeks to drive an evader, $\boldsymbol{E}$, into a target set ($\mathcal{L}_0$) or tube, $\mathcal{L}[[-T, 0], \mathcal{L}_0]$.

[3] The functional $\boldsymbol{\Phi}$ may be considered a functional mapping from an infinite-dimensional space to the space of real numbers.

[4] The definition of murmurations we use here has a semblance to the murmurations of possibly thousands of starlings observed in nature.

3.1 Backward Reachability from Differential Games Optimal Control

Backward reachability consists in avoiding an unsafe set of states under the worst-possible disturbance and at all times. The verification problem may consist in finding a *set of reachable states* that lie along the trajectories of the solution to a first order nonlinear P.D.E. that originates from some initial state $\boldsymbol{x}_0 = \boldsymbol{x}(0)$ up to a specified time bound, $t = t_f$: *from a set of initial and unsafe state sets, the time-bounded safety verification problem is to determine if there is an initial phase that the solution to the P.D.E. enters an unsafe set*. Backward reachable sets (BRS) or tubes (BRTs) are popularly analyzed as a game of two vehicles with non-stochastic dynamics [26]. Such BRTs possess discontinuity at cross-over points (which exist at edges) on the surface of the tube, and may be non-convex. In general, we seek for a *terminal payoff* $g(\cdot) : \mathbb{R}^n \to \mathbb{R}$ to satisfy

$$|g(\boldsymbol{x}(t))| \leq k, \quad |g(\boldsymbol{x}(t)) - g(\hat{\boldsymbol{x}(t)}) \mid \leq k|\boldsymbol{x}(t) - \hat{\boldsymbol{x}}(t) \mid \tag{1}$$

for constant k and all $T \leq t \leq 0$, $\hat{\boldsymbol{x}}$, $\boldsymbol{x} \in \mathbb{R}^n$, $\boldsymbol{u} \in \mathcal{U}$ and $\boldsymbol{v} \in \mathcal{V}$.

Now, suppose that a pursuer's mapping strategy (starting at t) is $\beta : \bar{\mathcal{U}}(t) \to \bar{\mathcal{V}}(t)$ provided for each $t \leq \tau \leq T$ and $\boldsymbol{u}(t), \hat{\boldsymbol{u}}(t) \in \bar{\mathcal{U}}(t)$; then $\boldsymbol{u}(\bar{t}) = \hat{\boldsymbol{u}}(\bar{t})$ a.e. on $t \leq \bar{t} \leq \tau$ implies $\beta[\boldsymbol{u}](\bar{t}) = \beta[\hat{\boldsymbol{u}}](\bar{t})$ a.e. on $t \leq \bar{t} \leq \tau$. Suppose further that the player $\boldsymbol{P}$ is controlling the strategy β and minimizing, while the player $\boldsymbol{E}$ is controlling its strategy, α, and maximizing. For any admissible control-disturbance pair $(\boldsymbol{u}(\cdot), \boldsymbol{v}(\cdot))$ and initial phase $(\boldsymbol{x}_0, t_0)$, Crandall [8] and Evan's [6] claim is that there exists a unique trajectory, $\boldsymbol{\xi}(t)$, the motion of the dynamical system, (3), passing through phase $(\boldsymbol{x}_0, t_0)$ under the action of control $\boldsymbol{u}$, and a worst-possible disturbance $\boldsymbol{v}$, and observed at a time t afterwards i.e.

$$\boldsymbol{\xi}(t) = \boldsymbol{\xi}(t; t_0, \boldsymbol{x}_0, \boldsymbol{u}(\cdot), \boldsymbol{v}(\cdot)). \tag{2}$$

Equation (2) is a solution of the following dynamical system, represented as a first-order p.d.e.

$$\dot{\boldsymbol{x}}(\tau) = f(\tau, \boldsymbol{x}(\tau), \boldsymbol{u}(\tau), \boldsymbol{v}(\tau)) \quad T \leq \tau \leq t, \quad \boldsymbol{x}(t) = \boldsymbol{x}, \tag{3}$$

almost everywhere (a.e.); where $f(\tau, \cdot, \cdot, \cdot)$ and $\boldsymbol{x}(\cdot)$ are bounded and Lipschitz continuous. This bounded Lipschitz continuity property assures uniqueness of the system response $\boldsymbol{x}(\cdot)$ to controls $\boldsymbol{u}(\cdot)$ and $\boldsymbol{v}(\cdot)$ [11]. a.e. with the property that

$$\boldsymbol{\xi}(t_0) = \boldsymbol{\xi}(t_0; t_0, \boldsymbol{x}_0, \boldsymbol{u}(\cdot), \boldsymbol{v}(\cdot)) = \boldsymbol{x}_0. \tag{4}$$

In backward reachability analysis, the lower value of the differential game [11] is used in constructing an analysis of the backward reachable set (or tube). The differential game's lower value for a solution $\boldsymbol{x}(t)$ that solves (3) for $\boldsymbol{u}(t)$ and $\boldsymbol{v}(t) = \beta[\boldsymbol{u}](\cdot)$ is used in backward reachability analysis, given as

$$\begin{aligned} \boldsymbol{V}^{-}(\boldsymbol{x}, t) &= \inf_{\beta \in \mathcal{B}(t)} \sup_{\boldsymbol{u} \in \mathcal{U}(t)} \boldsymbol{\Phi}(\boldsymbol{u}, \beta[\boldsymbol{u}]) \\ &= \inf_{\beta \in \mathcal{B}(t)} \sup_{\boldsymbol{u} \in \mathcal{U}(t)} \int_t^T l(\tau, \boldsymbol{x}(\tau), \boldsymbol{u}(\tau), \beta[\boldsymbol{u}](\tau)) d\tau + g\left(\boldsymbol{x}(T)\right). \end{aligned} \tag{5}$$

Lemma 1. *The backward reachability problem on the resolution of the infimum-supremum over the non-anticipative strategies of $\boldsymbol{P}$ and the controls of $\boldsymbol{E}$ with the time of capture resolved as an extremum of the cost functional over a time interval is given by*

$$\frac{\partial \boldsymbol{V}^-}{\partial t}(\boldsymbol{x},t) + \min\{0, \boldsymbol{H}^-(t;\boldsymbol{x},\boldsymbol{u},\boldsymbol{v},\boldsymbol{V}^-_{\boldsymbol{x}})\} = 0,\ \boldsymbol{x}\in\mathbb{R}^n, t\in[-T,0] \tag{6a}$$

$$\boldsymbol{V}^-(\boldsymbol{x},0) = g(\boldsymbol{x}), \tag{6b}$$

$$\textit{where } \boldsymbol{H}^-(t;\boldsymbol{x},\boldsymbol{u},\boldsymbol{v},p) = \max_{u\in\mathcal{U}}\min_{v\in\mathcal{V}}\langle f(t;\boldsymbol{x},\boldsymbol{u},\boldsymbol{v}),p\rangle, \tag{6c}$$

and p, the co-state, is the spatial derivative of $\boldsymbol{V}^-$ w.r.t $\boldsymbol{x}$. where the vector field $\boldsymbol{V}^-_{\boldsymbol{x}}$ is known in terms of the game's terminal conditions so that the overall game is akin to a two-point boundary-value problem.

Henceforward, for ease of readability, we will remove the minus superscript on the lower value and Hamiltonian (6c).

Proof. Lemma 1 is an adaptation of [12]. □

In the sentiment of [12], we say the zero sublevel set of $g(\cdot)$ in (6) i.e. $\mathcal{L}_0 = \{\boldsymbol{x}\in\bar{\Omega}\,|\,g(\boldsymbol{x})\leq 0\}$, is the *target set* in the phase space $\Omega\times\mathbb{R}$ for a backward reachability problem [27]. This target set[5] can represent the failure set, regions of danger, or obstacles to be avoided e.t.c. in the vectogram. And the *robustly controlled backward reachable tube* for $\tau\in[-T,0]$[6] is the closure of the open set

$$\begin{aligned}\mathcal{L}([\tau,0],\mathcal{L}_0) = \{\boldsymbol{x}\in\Omega\,|\,\exists\,\beta\in\bar{\mathcal{V}}(t)\,\forall\,\boldsymbol{u}\in\mathcal{U}(t),\exists\,\bar{t}\in[-T,0],\\ \boldsymbol{\xi}(\bar{t})\in\mathcal{L}_0\},\ \bar{t}\in[-T,0]\,.\end{aligned} \tag{7}$$

Read: the set of states from which the strategies β of $\boldsymbol{P}$, and for all controls $\mathcal{U}(t)$ of $\boldsymbol{E}$ imply that we reach the target set within the interval $[-T,0]$. More specifically, following Lemma 2 of [12], the states in the reachable set admit the following properties w.r.t the value function $\boldsymbol{V}$

$$\boldsymbol{x}\in\mathcal{L}_0 \implies \boldsymbol{V}^-(\boldsymbol{x},t)\leq 0 \text{ and } \boldsymbol{V}^-(\boldsymbol{x},t)\leq 0 \implies \boldsymbol{x}\in\mathcal{L}_0. \tag{8}$$

4 Materials and Methods.

We focus on the task verification problem, and we resolve the $(n-1)\in\mathbb{R}^n$-dimensional hypersurfaces or *interfaces* between flocks using level set methods [1]. Flocks F_j and F_k are separated by an interface. This interface is implicitly represented as a signed distance function $\boldsymbol{\Phi}(\boldsymbol{x})$ that is negative on the interior of one flock, and positive on interior of the other. The zero-level set $\boldsymbol{\Phi}(\boldsymbol{x})=0$ corresponds to the original interface $\boldsymbol{V}$ [28]. Adding time, the motion of the interface (the zero-level set) can then be described by an initial

[5] Note that the target set, $\mathcal{L}_0$, is a closed subset of $\mathbb{R}^n$ and is in the closure of Ω.
[6] The (backward) horizon, $-T$ is negative for $T>0$.

value problem that corresponds to a Cauchy-type Hamilton Jacobi partial differential equation [6, 8].

We locally synthesize the kinematics of agents in a manner amenable to state representation by resolving local payoff extremals – essentially a state space partition induced by a an aggregation of preexisting desired emergent collective behavior from local flocks[7]. Suppose that the local control laws are properly coordinated, the region of the state space across which their coordinated influence might be exerted constitute a larger e.g. *manipulability volume* for a dexterous kinematic task.

Assumptions: The many interacting subsystems under consideration employ (i) natural units of measurements that are the same for all agents; (ii) kinematics with linear speeds but with a capacity for orientation changes; (iii) intra-flock agent interaction is restricted within unique and distinct state space manifolds; and by agents maneuvering their direction, a kinematic alignment is obtained; (iv) inter-flock interaction occurs when a pursuer is within a threshold of capturing any agent within the murmuration.

Let us now formalize definitions that will aid the modularization of the problem into manageable forms.

Definition 1 (Neighbors of an Agent). *We define the neighbors $\mathcal{N}_i(t)$ of agent i at time t as the set of all agents that lie within a predefined radius, r_i, of agent i at time t. In every iteration of the game, we update an agent's neighbors as delineated in Algorithm 1.*

Definition 2. *We define a flock, F, consisting of agents labeled $\{1, 2, \cdots, n\}$ as a collection of agents within a phase space $(\mathcal{X}, T)$ such that all agents within the flock interact with their nearest neighbors in a topological sense.*

Remark 1. Every agent within a flock has similar dynamics to that of its neighbor(s). Furthermore, agents travel at the same linear speed, v; the angular headings, w, however, may be different between agents, seeing we are dealing with a many-bodied system. The state of an agent i within a flock j will be defined as $\boldsymbol{x}^{(i)_j}$ or $\boldsymbol{x}^i_j$. Each agent's continuous-time dynamics, $\dot{\boldsymbol{x}}^{(i)}(t)$, evolves as

$$\begin{bmatrix} \dot{\boldsymbol{x}}_1^{(i)}(t) \\ \dot{\boldsymbol{x}}_2^{(i)}(t) \\ \dot{\boldsymbol{x}}_3^{(i)}(t) \end{bmatrix} = \begin{bmatrix} v(t)\cos \boldsymbol{x}_3^{(i)}(t) \\ v(t)\sin \boldsymbol{x}_3^{(i)}(t) \\ \langle w^{(i)}(t) \rangle_r \end{bmatrix}, \langle w^{(i)}(t) \rangle_r = \frac{1}{1+n_i(t)} \left(w_i(t) + \sum_{j \in \mathcal{N}_i(t)} w_j(t) \right) \tag{9}$$

for agents $i = \{1, 2, 3, ..., n\}$, where t is the continuous-time index, $n_i(t)$ is the number of agent i's neighbors at time t, $\mathcal{N}_i(t)$ denotes the sets of labels of agent i's neighbors at time t, and $\langle w^{(i)}(t) \rangle_r$ is the average orientation of agent i w.r.t its neighbors at time t. Note that for a game where all agents share the same constant linear speed and heading, (9) reduces to the dynamics of a Dubins vehicle in absolute coordinates with

[7] Let the cursory reader understand that we use the concept of a flock loosely. The value function could represent a pallete of composed value functions whose extremals resolve local behaviors we would like to emerge over separated local regions of the state space of dextrous drone acrobatics [29], a robot balls juggling task [3] or any parallel task domain verification problem.

$-\pi \leq w^{(i)}(t) < \pi$. The averaging over the degrees of freedom of other agents in (9) is consistent with the *mean field theory*, whereby the effect of all other agents on any one agent is an approximation of a single averaged influence.

Definition 3 (Payoff of a Flock). *To every flock F_j (with a finite number of agents N) within a murmuration, $j = 1, 2, \cdots, m$, we associate a payoff, $\boldsymbol{\Phi}$, that is the union of all respective agent's payoffs for expressing the outcome of a desired kinematic behavior.*

Viscosity solutions provide a particular means of finding a unique solution with a clear interpretation in terms of the generalized optimal control problem, even in the presence of stochastic perturbations. Each agent within a flock interacts with a fixed number of neighbors, n_c, within a fixed topological range, r_c. This topological range is consistent with findings in collective swarm behaviors and it reinforces *group cohesion* [20]. However, we are interested in *robust group cohesion* in reachability analysis. Therefore, we let a pursuer, $\boldsymbol{P}$, with a worst-possible disturbance attack the flock, and we take it that flocks of agents constitute an evading player, $\boldsymbol{E}$. Returning to (9), for a single flock, we now provide a sketch for the HJI formulation for a heading consensus problem.

4.1 Framework for Separated Payoffs

We now make the following assumptions to enable our problem formulation. Suppose that a murmuration's global heading is predetermined and each agent i within each flock, F_j, $(j = 1, \cdots, n)$ in the murmuration has a constant linear velocity, v^i. An agent's orientation is its control input, given by the average of its own orientation and that of its neighbors. Instead of metric distance interaction rules that make agents very vulnerable to predators [20], we resort to a topological interaction rule[8].

What constitutes an agent's neighbors are computed based on empirical findings and studies from the lateral vision of birds and fishes [20, 21, 23] that provide insights into their anisotropic kinematic density and structure. Importantly, starlings' lateral visual axes and their lack of a rear sector reinforces their lack of nearest neighbors in the front-rear direction. As such, this enables them to maintain a tight density and robust heading during formation and flight. The algorithm for computing the nearest neighbors is given in Algorithm 1. On lines 3 and 7 of Algorithm 1, cohesion is reinforced by leveraging the observations above. While the neighbor updates for an agent involve an $O(n^2)$ algorithm in Algorithm 1, we are merely dealing with $6 - 7$ agents at a time in a local flock – making the computational cost measly.

Each agent within a flock F_j interacts with a fixed number of neighbors, n_c, within a fixed topological range, r_c[9]. This topological range is consistent with findings in collective swarm behaviors and it reinforces *group cohesion* [20]. However, we are interested in *robust group cohesion* in reachability analysis. Therefore, we let a pursuer,

[8] With metric distance rules, we will have to formulate the breaking apart of value functions that encode a consensus heading problem in order to resolve the extrema of multiple payoffs; which is typically what we want to mitigate against during real-world autonomous tasks.

[9] The topological range can be set as the distance between the labels of agents in a flock.

Algorithm 1 Nearest Neighbors For Agents in a Flock.

Given a set of agents $\boldsymbol{a} = \{a_1, a_2, \cdots, a_{n_a} \,|\, [a] = n_a\}$ ▷ n_a agents in a flock F_k.
function UPDATENEIGHBOR(n)
  for i in $1, \ldots, n$ **do** ▷ Look to the right and update neighbors.
    for j in $i+1, \ldots, n$ **do**
      COMPARE_NEIGHBOR($a[i]$, $a[j]$)
    end for
    for j in $i-1$ down to 0 **do** ▷ Look to the left and update neighbors.
      COMPARE_NEIGHBOR($a[i]$, $a[j]$)
    end for
  end for
  for each $a_i \in F_k$, $i = 1, \cdots n_a$ **do** ▷ Recursively update agents' headings.
    Update headings according to (9).
  end for
end function

function COMPARE_NEIGHBOR(a_1, a_2) ▷ (a_1, a_2): distinct instances of AGENT.
  if $|a_1$.label - a_2.label$| < a_1.r_c^1$ ▷ r_c^n: agent n's capture radius, r_c.
    a_1.UPDATE_NEIGHBORS(a_2) **then**
  end if
end function

procedure AGENT(a_i, Neighbors={}) ▷ Neighbors: Set of neighbors of this agent.
    ▷ Agent a_i with attributes label $\in \mathbb{N}$, avoid and capture radii, r_a, r_c.
  function UPDATE_NEIGHBORS(neigh)
    if length(neigh)> 1 **then** ▷ Multiple neighbors.
      for each neighbor of neigh **do**
        UPDATE_NEIGHBORS(neighbor) ▷ Recursive updates.
      end for
    end if
    Add neigh to Neighbors
  end function
end procedure

$\boldsymbol{P}$, with a worst-possible disturbance attack the flock, and we take it that flocks of agents constitute an evading player, $\boldsymbol{E}$.

4.2 Global Isotropy via Local Anisotropy

It has been observed that structural anisotropy is not merely an effect of a preferential velocity in animal flocking kinematics but rather an explicit effect of the anisotropic interaction character itself. By this theory, agents choose a mutual position on the state space in order to maximize the sensitivity to changes in heading and speed of neighbors as the neighbors' anisotropy is optimized and the scheme of avoiding collisions is vision-based but not related to the eye's structure [20].

Because of the robust group cohesion philosophy, we take it that at least one agent within a flock labeled j is under attack and is in relative coordinates with a pursuer, $\boldsymbol{P}^j$.

By averaging the heading of individual agents' orientations with its neighborsc.f. (9), individual agents within a flock can achieve fast response to danger when a pursuer is nearby. In this specialized case, capture does not necessarily occur, because the $\boldsymbol{E}$ and $\boldsymbol{P}$'s speeds and maximum turn radius are equal: if both players start the game with the same initial velocity and orientation, the relative equations of motion show that $\boldsymbol{E}$ can mimic $\boldsymbol{P}$'s strategy by forever keeping the starting radial separation. As such, the *barrier* is closed and the *game of kind* is to determine the surface [26]. However, owing to the high-dimensionality of the state space, we cannot resolve this barrier analytically, hence we resort to numerical approximation methods – in particular, we leverage a parallel Lax-Friedrichs integration scheme [7] which we implement in Cupy [30] in order to provide a *consistent* and *monotone* solution to the Hamiltonians of these HJI equations.

Therefore, for an agent i within a flock with index j in a murmuration, the equations of motion under attack from a predator p (see Fig. 2) in relative coordinates is

$$\begin{bmatrix} \dot{\boldsymbol{x}}_1^{(i)_j}(t) \\ \dot{\boldsymbol{x}}_2^{(i)_j}(t) \\ \dot{\boldsymbol{x}}_3^{(i)_j}(t) \end{bmatrix} = \begin{bmatrix} -v_e^{(i)_j}(t) + v_p^{(j)} \cos \boldsymbol{x}_3^{(i)_j}(t) + \langle w_e^{(i)_j} \rangle_r \boldsymbol{x}_2^{(i)_j}(t) \\ v_p^{(i)_j}(t) \sin \boldsymbol{x}_3^{(i)_j}(t) - \langle w_e^{(i)_j} \rangle_r \boldsymbol{x}_1^{(i)_j}(t) \\ w_p^{(j)}(t) - \langle w_e^{(i)_j}(t) \rangle_r \end{bmatrix} \text{ for } i = 1, \cdots, n_a \tag{10}$$

where n_a is the number of agents within a flock, $\left(\boldsymbol{x}_1^{(i)_j}(t), \boldsymbol{x}_2^{(i)_j}(t)\right) \in \mathbb{R}^2$, and we have $\boldsymbol{x}_3^{(i)_j}(t) \in [-\pi, +\pi)$[10]. Read $\boldsymbol{x}_1^{(i)_j}(t)$: the first component of the state of an agent i at time t which belongs to the flock j in the murmuration at time t. In absolute coordinates, the equation of motion for *free agents* is

$$\begin{bmatrix} \dot{\boldsymbol{x}}_1^{(i)_j}(t) \\ \dot{\boldsymbol{x}}_2^{(i)_j}(t) \\ \dot{\boldsymbol{x}}_3^{(i)_j}(t) \end{bmatrix} = \begin{bmatrix} v_e^{(i)_j}(t) \cos \boldsymbol{x}_3^{(i)_j}(t) \\ v_e^{(i)_j}(t) \sin \boldsymbol{x}_3^{(i)_j}(t) \\ \langle w_e^{(i)_j}(t) \rangle_r \end{bmatrix}. \tag{11}$$

As mentioned in Section 2, the evading player at anytime has controls $\{\boldsymbol{u}^1, \boldsymbol{u}^2, \cdots \boldsymbol{u}^n\}$ for agents $i = 1, \cdots, n$ completely under its will. Solving for such complex backward reach-avoid tube is akin to splitting the state space into a number of parts separated by surfaces.

4.3 Flock Motion from Aggregated Value Functions

We introduce the union operator i.e. $\bigcup$ below as an aggregation symbol since the respective payoffs of each agent in a flock may be implicitly or explicitly constructed on a grid[11] – when it is implicitly represented, say from a signed distance function, we shall aggregate the payoff of agents 1 and 2 as

$$\bigcup (\Phi_1(\boldsymbol{x}, t), \Phi_2(\boldsymbol{x}, t)) = \min(\Phi_1(\boldsymbol{x}, t), \Phi_2(\boldsymbol{x}, t)) \tag{12}$$

[10] We have multiplied the dynamics by -1 so that the extremal's resolution evolves backwards in time.

[11] In resolving the zero-level sets of HJ value functions, it is typical to represent the payoff's surface as the isocontour of some function (usually a signed distance function).

otherwise, other appropriate arithmetic or logical operation shall apply.

We assume that the *value* of a flock heading control (differential game) exists. And by an extension of Hamilton's principle of least action, the terminal motion of a flock coincide with the extremal of the payoff functional

$$\boldsymbol{V}(\boldsymbol{x},t) = \inf_{\beta^{(1)}\in\mathcal{B}^{(1)}} \sup_{\boldsymbol{u^{(1)}}\in\mathcal{U}^{(\infty)}(t)} \int_{t_0}^{t_f} l^{(1)}(t,\boldsymbol{x}^{(1)},\boldsymbol{u}^{(1)},\beta^{(1)}[\boldsymbol{u}^{(1)}])dt + g^{(1)}(\boldsymbol{x}(T)) \bigcup \cdots$$
$$\inf_{\beta^{(n)}\in\mathcal{B}^{(n)}(t)} \sup_{\boldsymbol{u}^{(n)}\in\mathcal{U}^{(n)}(t)} \int_{t_0}^{t_f} l^{(n)}(t,\boldsymbol{x}^{(1)},\boldsymbol{u}^{(1)},\boldsymbol{u}^{(n)},\beta^{(n)}[\boldsymbol{u}^{(n)}])dt + g^{(n)}(\boldsymbol{x}(T)) \tag{13}$$

where n is the total number of distinct flocks in a murmuration. The resolution of this equation admits a viscosity solution [6] to following variational terminal HJI PDE [12]

$$\bigcup_{i=1}^{n_f}\left[\bigcup_{i=1}^{n_a}\left(\frac{\partial \boldsymbol{V}_i}{\partial t}(\boldsymbol{x},t) + \min\left[0, \boldsymbol{H}^{(i)}(\boldsymbol{x}^{(i)}, \boldsymbol{V}_x(\boldsymbol{x},t))\right]\right)\right] = 0. \tag{14}$$

with Hamiltonian,

$$\boldsymbol{H}^{(i)}(t;\boldsymbol{x}^{(i)},\boldsymbol{u}^{(i)},\boldsymbol{v}^{(i)},p^{(i)}) = \max_{u^{(i)}\in\mathcal{U}^{(i)}} \min_{v^{(i)}\in\mathcal{V}^{(i)}} \langle f^{(i)}(t;\boldsymbol{x},\boldsymbol{u}^{(i)},\boldsymbol{v}^{(i)}), p^{(i)}\rangle. \tag{15}$$

In swarms' collective motion, when e.g. a Peregrine Falcon attacks, immediate nearest agents change direction almost instantaneously. And because of the interdependence of the orientations of individual agents with respect to one another, all other agents respond based on the nearest neighbor formulation of (9) and Line 3 of Algorithm 1, every agent in a murmuration responds accordingly. Thus, we only simulate a single attack against a flock within the murmuration to realize robust cohesion.

A pursuer can attack any flock within the murmuration from a distinct surface: a $\boldsymbol{P}$ direction: this side of the surface reached after penetration in the $\boldsymbol{P}-[\boldsymbol{E}-]$ direction is the $\boldsymbol{P}-[\boldsymbol{E}]$ *side* [25]. We attribute the term *in the small* to determine the smooth parts of the singular surface solution when a pursuer attacks, and when they are stitched together into the total solution, we shall describe them as *in the large*. There exists at least one value $\bar{\alpha}$ of α such that if $\alpha = \bar{\alpha}$, no vector in the β-vectogram[12] penetrates the surface in the E-direction. Similar arguments can be made for $\bar{\beta}$ which prevents penetration in the P-direction. We adopt [25]'s terminology and call these surfaces semi-permeable surfaces (SPS).

Throughout the game, we assume that the roles of $\boldsymbol{P}$ and $\boldsymbol{E}$ do not change, so that when capture can occur, a necessary condition to be satisfied by the saddle-point controls of the players is the Hamiltonian, $\boldsymbol{H}^i(\boldsymbol{x},p)$.

Theorem 1. *For a flock, F_j, the Hamiltonian is the total energy given by a summation of the exerted energy by each agent i so that we can write the main equation or total*

[12] A $\beta-$vectogram is the resulting state space when a the strategy β is applied in computing the optimal control law for an agent.

Hamiltonian of a murmuration as

$$\boldsymbol{H}(\boldsymbol{x},p) = \max_{w_e^{(k)^j}\in[\underline{w}_e^j,\bar{w}_e^j]} \min_{w_p^{(k)^j}\in[\underline{w}_p^j,\bar{w}_p^j]} \bigcup_{j=1}^{n_f} \left[H_a^{(k)^j}(\boldsymbol{x},p) \bigcup \left(\bigcup_{i=1}^{n_a-1} H_f^{(i)^j}(\boldsymbol{x},p) \right) \right] \tag{16}$$

$$\begin{aligned} &= \bigcup_{j=1}^{n_f} \left(\bigcup_{i=1}^{n_a-1} \left[p_1^{(i)^j} v^{(i)^j} \cos \boldsymbol{x}_3 + p_2^{(i)^j} v^{(i)^j} \sin \boldsymbol{x}_3 + p_3^{(i)^j} \langle w_e^{(i)^j} \rangle_r \right] \right. \\ &\quad \bigcup \left[p_1^{(k)^j} \left(v^{(k)^j} - v^{(k)^j} \cos \boldsymbol{x}_3^{(k)^j} \right) - p_2^{(k)^j} v^{(k)^j} \sin \boldsymbol{x}_3^{(k)^j} - \underline{w}_p^j |p_3^{(k)^j}| \right. \\ &\quad \left. \left. + \bar{w}_e^j \left| p_2^{(k)^j} \boldsymbol{x}_1^{(k)^j} - p_1^{(k)^j} \boldsymbol{x}_2^{(k)^j} + p_3^{(k)^j} \right| \right] \right). \end{aligned} \tag{17}$$

where $\boldsymbol{H}_a^{(k)^j}(\boldsymbol{x},p)$ is the Hamiltonian of the individual under attack by a pursuing agent, $\boldsymbol{P}$ and $H_f^{(i)^j}(\boldsymbol{x},p)$ are the respective Hamiltonians of the free agents, $i = 1,\cdots,n_f$, within an evading flock in a murmuration, and not under the direct influence of capture or attack by $\boldsymbol{P}$; we denote by $w_e^{(i)^j}$ the heading of an evader i within a flock j and $w_p^{(j)}$ the heading of a pursuer aimed at flock j; $\underline{w}_e^{(k)^j}$ is the orientation that corresponds to the orientation of the agent with minimum turn radius among all the neighbors of agent k, inclusive of agent k at time t; similarly, $\bar{w}_e^{(k)^j}$ is the maximum orientation among all of the orientation of agent k's neighbors.

Corollary 1. *For the special case where the linear speeds of the evading agents and pursuer are equal i.e. $v_e^{(i)^j}(t) = v_p(t) = +1m/s$, we have the Hamiltonian as*

$$\begin{aligned} \boldsymbol{H}(\boldsymbol{x},p) = \bigcup_{j=1}^{n_f} \left(\bigcup_{i=1}^{n_a-1} \left[p_1^{(i)^j} \cos \boldsymbol{x}_3 + p_2^{(i)^j} \sin \boldsymbol{x}_3 + p_3^{(i)^j} \langle w_e^{(i)^j} \rangle_r \right] \right. \\ \bigcup \left[p_1^{(k)^j} \left(1 - \cos \boldsymbol{x}_3^{(k)^j} \right) - p_2^{(k)^j} \sin \boldsymbol{x}_3^{(k)^j} - \underline{w}_p^j |p_3^{(k)^j}| \right. \\ \left. \left. + \bar{w}_e^j \left| p_2^{(k)^j} \boldsymbol{x}_1^{(k)^j} - p_1^{(k)^j} \boldsymbol{x}_2^{(k)^j} + p_3^{(k)^j} \right| \right] \right). \end{aligned} \tag{18}$$

We adopt the essentially non-oscillatory Lax-Friedrichs scheme of [14, 15] in resolving (18). Denote by (x,y,z) a generic point in $\mathbb{R}^3$ so that given mesh sizes Δx, Δy, Δz, $\Delta t > 0$, letters u,v,w will represent functions on the x,y,z lattice $\Delta = \{(x_i,y_j,z_k) : i,j,k \in \mathbb{Z}\}$. We define the numerical monotone flux, $\hat{\boldsymbol{H}}^{(i)^j}(\cdot)$, of $\boldsymbol{H}_j^{(i)}(\cdot)$ as

$$\begin{aligned} \hat{\boldsymbol{H}}^{(i)^j}(u^+,u^-,v^+,v^-,w^+,w^-) = \boldsymbol{H}^{(i)^j}\left(\frac{u^+ + u^-}{2}, \frac{v^+ + v^-}{2}, \frac{w^+ + w^-}{2} \right) \\ -\frac{1}{2}\left[\alpha_x^{(i)^j} \left(u^+ - u^- \right) + \alpha_y^{(i)^j} \left(v^+ - v^- \right) + \alpha_z^{(i)^j} \left(w^+ - w^- \right) \right] \end{aligned} \tag{19}$$

where

$$\alpha_x^{(i)_j} = \max_{\substack{a\leq u\leq b\\ c\leq v\leq d\\ e\leq w\leq f}} |\boldsymbol{H}_u^{(i)_j}(\cdot)|,\ \alpha_y^{(i)_j} = \max_{\substack{a\leq u\leq b\\ c\leq v\leq d\\ e\leq w\leq f}} |\boldsymbol{H}_v^{(i)_j}(\cdot)|,\ \alpha_z^{(i)_j} = \max_{\substack{a\leq u\leq b\\ c\leq v\leq d\\ e\leq w\leq f}} |\boldsymbol{H}_w^{(i)_j}(\cdot)|. \quad (20)$$

are dissipation coefficients, controlling the level of numerical viscosity in order to realize a stable solution that is physically realistic [14]. Here, the subscripts of $\boldsymbol{H}$ are the partial derivatives w.r.t the subscript variable, and the flux, $\hat{\boldsymbol{H}}(\cdot)$ is monotone for $a \leq u^{\pm} \leq b, c \leq v^{\pm} \leq d, e \leq w^{\pm} \leq f$. We adopt the total variation diminishing Runge-Kutta scheme of [31] in efficiently calculating essentially non-oscillating upwinding finite difference gradients of $\boldsymbol{H}(\cdot)$.

4.4 LargeBRAT as Chaining of Flockings' BRATs

The theory we propose here is inspired by the algorithmic notions of robust, self-organizing emergent "behaviors" such as those observed in unactuated masses with passive mechanical guideways [3] or murmurations.

- Chain backward in time, from a murmuration goal, to an attacked flocking's anisotropic heading direction [32] (Inspired from Nilsson 1980)
- Mumrmuration BRAT verification strategy construed as a sequence of guarded motions [**?**]
-

TO-DO: Under development.

5 Experiments

At issue is a family of games based on different starting points for local flocks that on the whole constitute a murmuration (see Fig. 3). In starlings, agents move in local flocks of six to seven nearest neighbors [20] in order to preserve cohesion and heading consensus. Therefore, we implicitly compute the payoff for each individual agent in every flock. In this light, a flock's payoff is a union (element-wise minimum f respective payoff points) of the payoff of every agent within it. Therefore, we define the target set and the tube as

$$\mathcal{L}_0 = \left\{\boldsymbol{x} \in \bar{\Omega} | \boldsymbol{V}(\boldsymbol{x},0) \leq 0, \boldsymbol{V}(\boldsymbol{x},0) = \boldsymbol{V}_1(\boldsymbol{x}_1,0) \bigcup \cdots \bigcup \boldsymbol{V}_n(\boldsymbol{x}_n,0)\right\}, \quad (21)$$
$$\mathcal{L}([\tau,0],\mathcal{L}_0) = \left\{\boldsymbol{x} \in \bar{\Omega} | \boldsymbol{V}(\boldsymbol{x},\tau) \leq 0, \boldsymbol{V}(\boldsymbol{x},0) = \boldsymbol{V}_1(\boldsymbol{x}_1,0) \bigcup \cdots \bigcup \boldsymbol{V}_n(\boldsymbol{x}_n,0)\right\}$$

where $\tau \in [-T, 0]$.

A pictorial representation of the zero-level robustly controllable backward reach-avoid tubes (RCBRAT) of various differential games with finite agents in the evading flock (c.f. Fig. 2)[13], constructed from a union of each agent's respective payoff, is depicted in Fig. 3. These are the aggregated payoffs of all agents that constitute each

[13] More results for other flocks are included in the appendix.

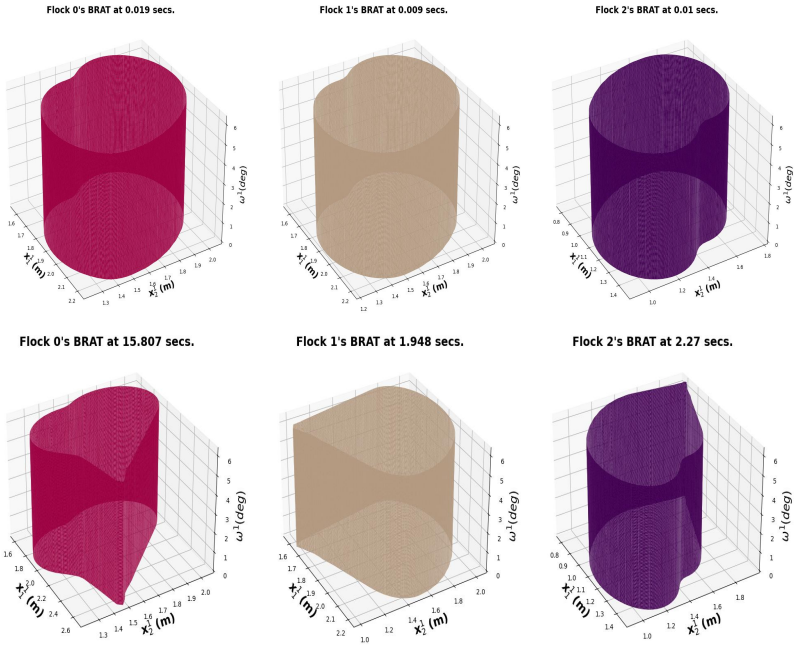

Fig. 3: Top: Initial zero-level set for a flock initialized from a specific initial condition. Bottom: Interface of the respective evading flock under attack from a pursuer at the end a Lax-Friedrichs' integration. (Metric reach radius=$0.2m$, Avoid Radius=$0.2m$). More results are included in the appendix B.

flock. Each agent's payoff is implicitly defined by a signed distance representation on the state space [33] i.e. ,

$$\boldsymbol{V}^{(i)}(\boldsymbol{x},0) = \sqrt{\boldsymbol{x}_1^{(i)^2} + \boldsymbol{x}_2^{(i)^2}} - r_c^{(i)} \tag{22}$$

where r_c is the capture radius. And the payoff for an evading flock is taken as the union of all individual agent's payoff as

$$\boldsymbol{V}_j(\boldsymbol{x},0) = \bigcup_{i=1}^{n_a} \sqrt{\boldsymbol{x}_1^{(i)^2} + \boldsymbol{x}_2^{(i)^2}} - r_c^{(i)} \tag{23}$$

In the original fronts propagation algorithm of [2], the zero-level set in embedded throughout the state space. This adds a lot of computational complexity to the computational procedure. To circumvent this, in each iteration of the numerical integration scheme, we compute the grid bounds of the zero-level set of an interface, and we update the state space with the newly constructed grid. This hastens computational time, by reducing the complexity of the numerical flux integration scheme to just the number of elements on the front.

Every local flock has its own payoff, whose target set, together with those of nearest neighbors being interacted with are related by the surfaces. The zero level set of the union

of these payoffs constitute the avoid set for a heading consensus. To ensure adequate spatial separation between every agent, we initialize a flock's j's agents, $i = 1, \ldots, n$ on the vectogram in the following way:

$$\boldsymbol{x}^{(i)_j} = \left[r_c \cos(\tfrac{i\pi}{4}),\, r_c \sin(\tfrac{i\pi}{4}),\, h + i\,\delta h \right]^T \tag{24}$$

where $h = 0.1$, $\delta h = 0.05$ and r_c is a collision avoidance radius.

We initialize each flock's agents to distinct positions on the vectogram. All agents share the same linear speed, v and their orientations, $\langle w^{(i)}(t) \rangle_r$, are averaged across every agent that falls within a nearest neighboring radius, r_i of the label of agent i. This is expressed on line 2 of Algorithm 1 . in a flock according to (9). Nearest neighbors are updated as described in Algorithm 1.

We want an adaptive allocation rule for the pursuer when aiming for an evading individual agent since in the process of hunting for a prey, an originally targeted prey may evade an attacker. We want the attacker to resort to redundant options so that anisotropy is enforced within a trajectory's evolution. Therefore, robust cohesion is reinforced by having an attacking pursuer randomly play against an evading flock in every iteration of the game as seen in Fig. 2.

Since the orientations of neighboring agents are averaged with that of the singled-out bird, the information is inevitably propagated across the entire flock, and hence the murmuration. We found a Courant-Friedrichs-Lax (CFL) factor of 0.65 to be a good hyperparameter during the integration of the HJI PDE(17). We adopt a warm-starting optimization scheme for the computation of the BRAT of each flock in our implementation so that we can leverage information accumulated during previous iterations when an optimization takes too long. We simply reload a BRAT from hard-disk from a different time step in the optimization process, and advance the Lax-Friedrichs integration scheme backward in time[14].

6 Conclusion

We have proposed an Hamilton-Jacobi-Isaacs systems verification scheme, based on Hamilton-Jacobi's reachability theory for constructing backward reachable tubes and sets for a complex system under the assumption that special local structures inherent within the system can enable the chaining of separately computed value function's zero-level sets.

One of the challenges we faced in our implementation is that the optimization scheme frequently halts at a local extrema of the solution landscape of the level set if the integration steps per iteration are rather coarse. To circumvent this, we employed fine numerical time step marching schemes. While this encourages further descent in the optimization per iteration, convergence is very slow. We will investigate this in a future work.

[14] An easier way to proceed backwards in time is to negate the dynamic equations in (9) and (10)

7 Acknowledgment

A rising vote of thanks to Professors Sylvia Herbert and Ian Abraham of the Mechanical and Aerospace Department of UC San Diego and Yale University respectfully for early feedback and discussions in the development of the ideas reported herein.

And special thanks to Cyril Zhang of Microsoft Research NYC for helping out with programming (code) parallelization across multiple graphical processing units.

References

1. Sethian, J.A.: Level Set Methods And Fast Marching Methods: Evolving Interfaces In Computational Geometry, Fluid Mechanics, Computer Vision, And Materials Science. Robotica **18**(1), 89–92 (2000) 1, 7
2. Osher, S., Sethian, J.A.: Fronts propagating with curvature-dependent speed: Algorithms based on hamilton-jacobi formulations. Journal of computational physics **79**(1), 12–49 (1988) 1, 15
3. Burridge, R R and Rizzi, A A and Koditschek, D E: Sequential Composition of Dynamically Dexterous Robot Behaviors. Tech. Rep. 6 (1999) 1, 8, 14
4. Brockett, R.W., et al.: Asymptotic Stability and Feedback Stabilization. Differential Geometric Control Theory **27**(1), 181–191 (1983) 1
5. Lions, P.L.: Generalized solutions of Hamilton-Jacobi equations, vol. 69. London Pitman (1982) 2
6. Evans, L., Souganidis, P.E.: Differential Games And Representation Formulas For Solutions Of Hamilton-Jacobi-Isaacs Equations. Indiana Univ. Math. J **33**(5), 773–797 (1984) 2, 6, 8, 12
7. Crandall, M.G., Evans, L.C., Lions, P.L.: Some Properties of Viscosity Solutions of Hamilton-Jacobi Equations. Transactions of the American Mathematical Society **282**(2), 487 (1984) 2, 11
8. Crandall, M.G., Lions, P.L.: Viscosity solutions of hamilton-jacobi equations. Transactions of the American mathematical society **277**(1), 1–42 (1983) 2, 6, 8
9. Lygeros, J.: On reachability and minimum cost optimal control. Automatica **40**(6), 917–927 (2004) 2
10. Mitchell, I.: A Robust Controlled Backward Reach Tube with (Almost) Analytic Solution for Two Dubins Cars. EPiC Series in Computing **74**, 242–258 (2020) 2, 3
11. Evans, L., Souganidis, P.E.: Differential games and representation formulas for solutions of Hamilton-Jacobi-Isaacs equations. Indiana Univ. Math. J **33**(5), 773–797 (1984) 2, 6
12. Mitchell, I.M., Bayen, A.M., Tomlin, C.J.: A time-dependent Hamilton-Jacobi formulation of reachable sets for continuous dynamic games. IEEE Transactions on Automatic Control **50**(7), 947–957 (2005). DOI 10.1109/TAC.2005.851439 2, 7, 12
13. Crandall, M.G., Majda, A.: Monotone Difference Approximations For Scalar Conservation Laws. Mathematics of Computation **34**(149), 1–21 (1980) 2
14. Crandall, M.G., Lions, P.L.: Two Approximations of Solutions of Hamilton-Jacobi Equations. Mathematics of Computation **43**(167), 1 (1984) 2, 3, 13, 14
15. Osher, S., Shu, C.W.: High-Order Essentially Nonoscillatory Schemes for Hamilton-Jacobi Equations. SIAM Journal of Numerical Analysis **28**(4), 907–922 (1991) 2, 3, 13
16. Herbert, S., Choi, J.J., Sanjeev, S., Gibson, M., Sreenath, K., Tomlin, C.J.: Scalable learning of safety guarantees for autonomous systems using hamilton-jacobi reachability. arXiv preprint arXiv:2101.05916 (2021) 2
17. Bajcsy, A., Bansal, S., Bronstein, E., Tolani, V., Tomlin, C.J.: An Efficient Reachability-based Framework for Provably Safe Autonomous Navigation in Unknown Environments. In: 2019 IEEE 58th Conference on Decision and Control (CDC), pp. 1758–1765. IEEE (2019) 2
18. Bansal, S., Tomlin, C.J.: DeepReach : A Deep Learning Approach to High-Dimensional Reachability 2
19. Cavagna, A., Cimarelli, A., Giardina, I., Parisi, G., Santagati, R., Stefanini, F., Viale, M.: Scale-ffee correlations in starling flocks. Proceedings of the National Academy of Sciences **107**(26), 11,865–11,870 (2010) 3
20. Ballerini, M., Cabibbo, N., Candelier, R., Cavagna, A., Cisbani, E., Giardina, I., Lecomte, V., Orlandi, A., Parisi, G., Procaccini, A., Viale, M., Zdravkovic, V.: interaction Ruling Animal

Collective Behavior Depends On Topological Rather Than Metric Distance: Evidence From A Field Study. Proceedings of the National Academy of Sciences **105**(4), 1232–1237 (2008). DOI 10.1073/pnas.0711437105. URL https://www.pnas.org/content/105/4/1232 3, 9, 10, 14
21. Helbing, D., Farkas, I., Vicsek, T.: Simulating dynamical features of escape panic. Nature **407**(6803), 487–490 (2000) 3, 9
22. Vicsek, T., Czirók, A., Ben-Jacob, E., Cohen, I., Shochet, O.: Novel type of phase transition in a system of self-driven particles. Physical review letters **75**(6), 1226 (1995) 3
23. Jadbabaie, A., Lin, J., Morse, A.S.: Coordination of groups of mobile autonomous agents using nearest neighbor rules. IEEE Transactions on automatic control **48**(6), 988–1001 (2003) 3, 9
24. Haiken, M.: These birds flock in mesmerizing swarms of thousandsbut why is still a mystery. (2021). URL https://www.nationalgeographic.com/animals/article/these-birds-flock-in-mesmerizing-swarms-why-is-still-a-mystery 3
25. Isaacs, R.: Differential games 1965. Kreiger, Huntigton, NY 5, 12
26. Merz, A.: The game of two identical cars. Journal of Optimization Theory and Applications **9**(5), 324–343 (1972) 6, 11, 20
27. Mitchell, I.: Games of two identical vehicles. Dept. Aeronautics and Astronautics, Stanford Univ., ... (July), 1–29 (2001). URL http://www.cs.ubc.ca/$\sim$mitchell/Papers/merz.pdf 7
28. Sethian, J.A.: Numerical Methods for Propagating Fronts. In: Variational methods for free surface interfaces, pp. 155–164. Springer (1987) 7
29. Kaufmann, E., Loquercio, A., Ranftl, R., Müller, M., Koltun, V., Scaramuzza, D.: Deep Drone Acrobatics. arXiv preprint arXiv:2006.05768 (2020) 8
30. Nishino, R., Loomis, C., Hido, S.: Cupy: A numpy-compatible library for nvidia gpu calculations. 31st confernce on neural information processing systems **151** (2017) 11
31. Osher, S., Shu, C.W.: Efficient Implementation of Essentially Non-Oscillatory Shock Capturing Schemes. Tech. rep., NASA Langley Research Center, Hampton, Virginia (1987) 14
32. Lozano-Perez, T., Mason, M.T., Taylor, R.H.: Automatic Synthesis of Fine-Motion Strategies for Robots. The International Journal of Robotics Research **3**(1), 3–24 (1984) 14
33. Osher, S., Fedkiw, R.: Level Set Methods and Dynamic Implicit Surfaces. Applied Mechanics Reviews **57**(3), B15–B15 (2004) 15, 20

A Hamiltonian of a Murmuration

In this appendix, we provide a derivation for the Hamiltonian of a flock, and by extension, that of a murmuration. In our implementations, the zero-level set is constructed implicitly from the isocontour of a signed distance function as described in [33, Chapter II].

Recall from (17) that the total Hamiltonian of a flock is a union of the mechanical energy of the free agents in a flock and the individual under attack i.e.

$$\boldsymbol{H}(\boldsymbol{x},p) = \max_{w_e^{(k)^j}\in[\underline{w}_e^j,\bar{w}_e^j]} \min_{w_p^{(k)^j}\in[\underline{w}_p^j,\bar{w}_p^j]} \bigcup_{j=1}^{n_f} \left[H_a^{(k)^j}(\boldsymbol{x},p) \bigcup \left(\bigcup_{i=1}^{n_a-1} H_f^{(i)^j}(\boldsymbol{x},p) \right) \right] \tag{25}$$

Proof of Theorem 1. We write the Hamiltonian of the free agents in absolute coordinates and the Hamiltonian of the agent under attack in relative coordinates with respect to the pursuer. A flock's Hamiltonian is Hamiltonian of the free agents is the aggregation of all the mechanical energy in the system in absolute coordinates i.e.

$$\bigcup_{i=1}^{n_a-1} H_f^{(i)^j}(\boldsymbol{x},p) = \bigcup_{i=1}^{n_a-1} \begin{bmatrix} p_1^{(i)^j} & p_3^{(i)^j} & p_3^{(i)^j} \end{bmatrix} \begin{bmatrix} v^{(i)^j}\cos\boldsymbol{x}_3 \\ v^{(i)^j}\sin\boldsymbol{x}_3 \\ \langle w_e^{(i)^j}\rangle_r \end{bmatrix} \tag{26}$$

where we have again dropped the time arguments for convenience. It follows that

$$\bigcup_{i=1}^{n_a-1} H_f^{(i)^j}(\boldsymbol{x},p) = \bigcup_{i=1}^{n_a-1} \left[p_1^{(i)^j}\, v^{(i)^j}\cos\boldsymbol{x}_3 + p_3^{(i)^j}\, v^{(i)^j}\sin\boldsymbol{x}_3 + p_3^{(i)^j}\,\langle w_e^{(i)^j}\rangle_r \right]. \tag{27}$$

Equation (17) can be re-written as

$$\begin{aligned} \boldsymbol{H}_a^{(k)^j}(\boldsymbol{x},p) = -\Bigg(\max_{w_e^{(k)^j}\in[\underline{w}_e^j,\bar{w}_e^j]} \min_{w_p^{(k)^j}\in[\underline{w}_p^j,\bar{w}_p^j]} & \begin{bmatrix} p_1^{(k)^j}(t) & p_2^{(k)^j}(t) & p_3^{(k)^j}(t) \end{bmatrix} \\ & \begin{bmatrix} -v_e^{(k)^j}(t) + v_p^{(j)}\cos\boldsymbol{x}_3^{(k)^j}(t) + \langle w_e^{(k)^j}\rangle_r(t)\boldsymbol{x}_2^{(k)^j}(t) \\ v_p^j(t)\sin\boldsymbol{x}_3^{(k)^j}(t) - \langle w_e^{(k)^j}\rangle_r(t)\boldsymbol{x}_1^{(k)^j}(t) \\ w_p^j(t) - \langle w_e^{(k)^j}(t)\rangle_r \end{bmatrix} \Bigg), \end{aligned} \tag{28}$$

where $p_l^{(k)^j}(t)\ |_{l=1,2,3}$ are the adjoint vectors [26]. For the pursuer, its minimum and maximum turn rates are fixed so that we have $\underline{w}_p^j$ as the minimum turn bound of the pursuing vehicle, and $\bar{w}_p^j$ is the maximum turn bound of the pursuing vehicle. Henceforth, we drop the templated time arguments for ease of readability. Rewriting (28), we find

that

$$\boldsymbol{H}_a^{(k)_j}(\boldsymbol{x},p) = -\left(\max_{w_e^{(k)_j}\in[\underline{w}_e^j,\bar{w}_e^j]}\min_{w_p^{(k)_j}\in[\underline{w}_p^j,\bar{w}_p^j]}\left[-p_1^{(k)_j}v_e^{(k)_j}+p_1^{(k)_j}v_p^j\cos\boldsymbol{x}_3^{(k)_j}\right.\right.$$
$$\left.\left.+p_1^{(k)_j}\langle w_e^{(k)_j}\rangle_r\boldsymbol{x}_2^{(k)_j}+p_2^{(k)_j}v_p^j\sin\boldsymbol{x}_3^{(k)_j}-p_2^{(k)_j}\langle w_e^{(k)_j}\rangle_r\boldsymbol{x}_1^{(i)_j}+p_3^{(k)_j}\left(w_p^j-\langle w_e^{(k)}\rangle_r\right)\right]\right),$$
$$=p_1^{(k)_j}\left(v_e^{(k)_j}-v_p^j\cos\boldsymbol{x}_3^{(k)_j}\right)-p_2^{(k)_j}v_p^j\sin\boldsymbol{x}_3^{(k)_j}$$
$$+\left(\max_{\langle w_e^{(k)_j}\rangle_r\in[\underline{w}_e^j,\bar{w}_e^j]}\min_{w_p^j\in[\underline{w}_p^j,\bar{w}_p^j]}\left[\langle w_e^{(k)_j}\rangle_r\left(p_2^{(k)_j}\boldsymbol{x}_1^{(k)_j}-p_1^{(k)_j}\boldsymbol{x}_2^{(k)_j}+p_3^{(k)_j}\right)-p_3^{(k)_j}w_p^j\right]\right). \tag{29}$$

It follows that we have from (29) that

$$\boldsymbol{H}_a^{(k)_j}(\boldsymbol{x},p) = p_1^{(k)_j}\left(v_e^{(k)_j}-v_p^j\cos\boldsymbol{x}_3^{(k)_j}\right)-p_2^{(k)_j}v_p^j\sin\boldsymbol{x}_3^{(k)_j}-\underline{w}_p^j|p_3^{(k)_j}|$$
$$+\bar{w}_e^j\left|p_2^{(k)_j}\boldsymbol{x}_1^{(k)_j}-p_1^{(k)_j}\boldsymbol{x}_2^{(k)_j}+p_3^{(k)_j}\right| \tag{30}$$

and that

$$\boldsymbol{H}_f^{(i)_j}(\boldsymbol{x},p) = \left[p_1^{(i)_j}\,v^{(i)_j}\cos\boldsymbol{x}_3+p_3^{(i)_j}\,v^{(i)_j}\sin\boldsymbol{x}_3+p_3^{(i)_j}\,\langle w_e^{(i)_j}\rangle_r\right]. \tag{31}$$

A fortiori the main equation (17) becomes

$$\boldsymbol{H}(\boldsymbol{x},p) = \bigcup_{j=1}^{n_f}\left(\bigcup_{i=1}^{n_a-1}\left[p_1^{(i)_j}\,v^{(i)_j}\cos\boldsymbol{x}_3+p_2^{(i)_j}\,v^{(i)_j}\sin\boldsymbol{x}_3+p_3^{(i)_j}\,\langle w_e^{(i)_j}\rangle_r\right]\right.$$
$$\left.\bigcup\left[p_1^{(k)_j}\left(v^{(k)_j}-v^{(k)_j}\cos\boldsymbol{x}_3^{(k)_j}\right)-p_2^{(k)_j}v^{(k)_j}\sin\boldsymbol{x}_3^{(k)_j}-\underline{w}_p^j|p_3^{(k)_j}|\right.\right.$$
$$\left.\left.+\bar{w}_e^j\left|p_2^{(k)_j}\boldsymbol{x}_1^{(k)_j}-p_1^{(k)_j}\boldsymbol{x}_2^{(k)_j}+p_3^{(k)_j}\right|\right]\right). \tag{32}$$

For the special case where the linear speeds of the evading agents and pursuer are equal i.e. $v_e^{(i)_j}(t)=v_p(t)=+1m/s$, we have a murmuration's Hamiltonian as

$$\boldsymbol{H}(\boldsymbol{x},p) = \bigcup_{j=1}^{n_f}\left(\bigcup_{i=1}^{n_a-1}\left[p_1^{(i)_j}\,\cos\boldsymbol{x}_3+p_2^{(i)_j}\,\sin\boldsymbol{x}_3+p_3^{(i)_j}\,\langle w_e^{(i)_j}\rangle_r\right]\right.$$
$$\left.\bigcup\left[p_1^{(k)_j}\left(1-\cos\boldsymbol{x}_3^{(k)_j}\right)-p_2^{(k)_j}\sin\boldsymbol{x}_3^{(k)_j}-\underline{w}_p^j|p_3^{(k)_j}|\right.\right.$$
$$\left.\left.+\bar{w}_e^j\left|p_2^{(k)_j}\boldsymbol{x}_1^{(k)_j}-p_1^{(k)_j}\boldsymbol{x}_2^{(k)_j}+p_3^{(k)_j}\right|\right]\right). \tag{33}$$

□

B Flocks' Robustly Controllable BRATs

Note that the symmetry between non-consecutive flock labels e.g. flock 1 and flock 3's RCBRAT is because the we multiplied the initial position of a flock's state by -1.

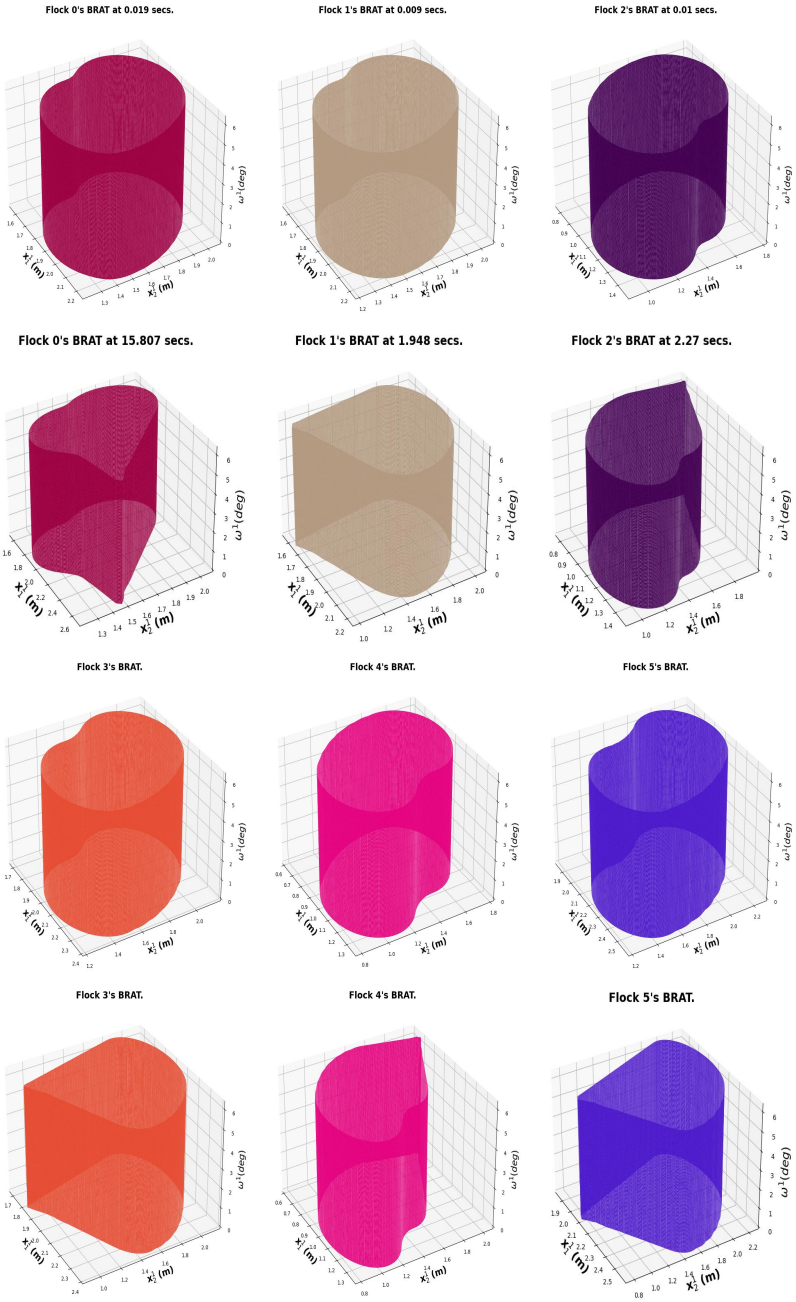

Fig. 4: Top Rows: Initial zero-level set for flocks initialized from different initial conditions. Bottom: Interface of the respective evading flock under attack from a pursuer after specific Lax-Friedrichs' integration. (Metric reach radius=$0.2m$, Avoid Radius=$0.2m$).